Hindawi Publishing Corporation
Journal of Nanomaterials
Volume 2015, Article ID 673135, 6 pages
http://dx.doi.org/10.1155/2015/673135

Research Article

Effect of CdS/Mg-Doped CdSe Cosensitized Photoanode on Quantum Dot Solar Cells

Yingxiang Guan, Xiaoping Zou, and Sheng He

Research Center for Sensor Technology, Beijing Key Laboratory for Sensor, Ministry of Education Key Laboratory for Modern Measurement and Control Technology, School of Applied Sciences, and School of Information & Communication Engineering, Beijing Information Science and Technology University, Jianxiangqiao Campus, Beijing 100101, China

Correspondence should be addressed to Xiaoping Zou; xpzou2005@gmail.com

Received 31 May 2014; Accepted 13 August 2014

Academic Editor: Yongfeng Li

Quantum dots have emerged as a material platform for low-cost high-performance sensitized solar cells. And doping is an effective method to improve the performance of quantum dot sensitized solar cells (QDSSCs). Since Kwak et al. from South Korea proved the incorporation of Mg in the CdSe quantum dots (QDs) in 2007, the Mg-doped CdSe QDs have been thoroughly studied. Here we report a new attempt on CdS/Mg-doped CdSe quantum dot cosensitized solar cells (QDCSSC). We analyzed the performance of CdS/Mg-doped CdSe quantum dot cosensitized solar cells via discussing the different doping concentration of Mg and the different SILAR cycles of CdS. And we studied the mechanism of CdS/Mg-doped CdSe QDs in detail for the reason why the energy conversion efficiency had been promoted. It is a significant instruction on the development of Mg-doped CdSe quantum dot sensitized solar cells (QDSSCs).

1. Introduction

Recently, doping of semiconductor quantum dot has been largely developed. It provides a broad way to achieve low-cost high-performance optoelectronic devices. Lee and his colleagues reported on a PbS:Hg QDSSC with high power conversion of 5.6% for the extremely high J_{sc} (30 mA/cm^2) last year [1]. It has shown the great potential of QDSSCs. CdSe is a kind of sensitizer system and has gotten lots of research. Mg-doped CdSe is one kind of doping scheme. In 2007, Kwak et al. proved that Mg was doped into CdSe with X-ray energy dispersive spectroscopy (EDS) and inductively coupled plasma mass spectrometry (ICPMS) [2]. And they adjusted the band-gap of CdSe nanocrystalline by doping CdSe with Mg which was blue shifted and the intensity of PL spectra of doped CdSe nanocrystalline was similar with that of undoped CdSe nanocrystalline, or even higher. Then they enhanced the ripening kinetics of Mg-doped CdSe nanocrystals because of the low activation energy for the volume diffusion [3]. In 2008, Wonjoo et al. prepared CdSe/Mg-doped CdSe QDSSCs with chemical bath deposition (CBD) method [4]. It had a more broad range of spectral response in visible region. Thus, the short-circuit current was enhanced by 47%, but the fill factor (FF) and the open circuit voltage did not change significantly compared with undoped CdSe QDSSCs. In 2010, Wang et al. from Qufu Normal University announced the first-principles on the electron structure and optical properties of Mg-doped CdSe system [5]. They calculated the electron structure and optical properties of wurtzite structure $Cd_{1-x}Mg_xSe$ ($x = 0, 0.125, 0.250, 0.375$) by using first-principles ultrasoft pseudopotential plane wave method based on the density functional theory (DFT). The result showed that Se4p electrons fundamentally determined the top of valence band which was essentially the same, while both Se4s electrons and Cd5s electrons determined the bottom of conduction band which was moved to a higher energy region with the increasing Mg concentration, and the band-gap was also broadened. As a result, the peaks in the imaginary part of the dielectric function and the peak in the real part of the refractive index were blue shifted with the

increasing Mg concentration. The CdS/CdSe system is one of the most studied systems. Lee et al. achieved an energy conversion efficiency of 4.22% by using a TiO_2/CdS/CdSe/ZnS electrode structure in 2009 [6]. Because of the Fermi level alignment, a stepwise structure of band-edge levels was yielded in the cascade structure of TiO_2/CdS/CdSe electrode. And it profited the electron injection and hole recovery.

As we were enlightened by the previous research on doping [7–9] of our research group and the research on Mg-doped CdSe and CdS/CdSe photoanode structure of others, we report a quantum dot cosensitized solar cell prepared by using successive ionic layer absorption and reaction (SILAR) method based on cosensitized CdS/Mg-doped CdSe QDs. (Mg-CdSe stands for Mg-doped CdSe.)

2. Methods

2.1. Device Fabrication. Firstly, with regard to TiO_2 films fabrication, TiO_2 films were printed on the cleaned FTO glass which was treated by a 0.4 M $TiCl_4$ solution and then annealed at 450°C for 30 min with screen printing method and then annealed at 450°C for 30 min. The thickness of TiO_2 films was about 8.5 μm and the working area was $0.5 \times 0.5\,cm^2$. Secondly, in photoanode fabrication,the TiO_2 films were dipped into a $Cd(NO_3)_2$ ethanol solution (0.1 M) for 5 min and then rinsed with ethanol. After being dried with nitrogen they were dipped into a Na_2S methanol solution (0.1 M) for 5 min and then rinsed with methanol. The two steps were termed as one SILAR cycle. It was similar to the deposition of Mg-CdSe QDs; the cation solution was prepared by adding the $MgCl_2{\cdot}6H_2O$ into preceding Cd^{2+} solution with a settled molar concentration ratio. The anion solution (Na_2SeSO_3) was prepared by refluxing Se (0.06 M) into a Na_2SO_3 aqueous solution (0.12 M) at 70°C for 7 h. But there were longer time (ca. 30 min) and higher temperature (50°C) for dipping them into anion solution. Thirdly, in counter electrode fabrication, Pt counter electrode was prepared by thermal decomposition of chloroplatinic acid; the method is as follows: 0.053 g chloroplatinic acid was dissolved in 10 mL isopropanol to fabricate platinum paste. Then, the Pt counter electrode could be obtained by annealing the FTO glass which was coated with the platinum paste in Muffle furnace at 450°C for 30 min. Fourthly in electrolyte preparation,polysulfide electrolyte was prepared by dissolving 1 M Na_2S and 1 M S in deionized water. Finally, with regard to cells packaging, the prepared photoanode was put on laboratory bench (the coated side facing up). Next a hollow rectangle spacer with the thickness of 60 μm was placed around the photoanode. Then the prepared Pt counter electrode (the conductive side facing down) was put on the photoanode. Then the electrolyte was injected into the cell from the gap between photoanode and counter electrode followed by griping the cell with clips. (Finished cell should be placed under dark for 40 min before testing.)

2.2. Material Characterization. Scanning electron microscopy (SEM) was used to observe the surface of the films. SEM was performed with a S-4300 of Technical Institute of Physics and Chemistry, CAS. Energy dispersive X-ray spectroscopy (EDS) was employed with S-4300 equipped with a high-performance energy dispersive X-ray spectroscopy (EDS). Transmission electron microscopy (TEM) was measured with Tecnai G2 F20 S-TWIN at 200 KV. X-ray diffraction (XRD) was performed with Bruker D8 focus. Absorption spectra were measured with a Varian Cary 5000 UV-Vis spectrophotometer. Inductively coupled plasma optical emission spectroscopy (ICP-IOS) analysis was performed with a Thermo Fisher IRIS Intrepid II XSP.

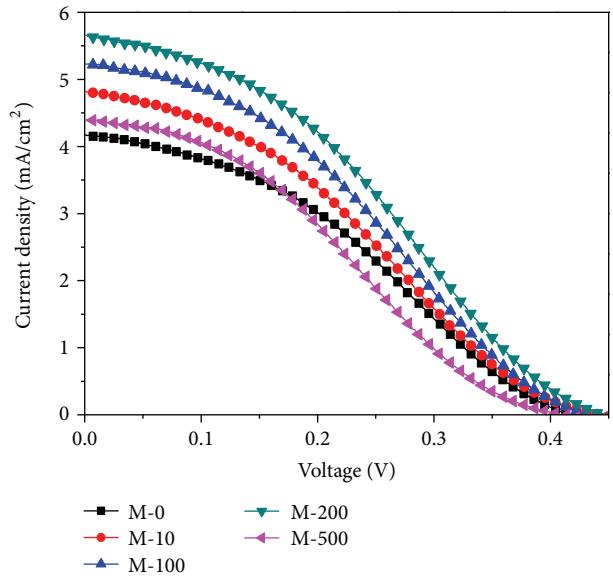

Figure 1: The J-V curves of the cells made by sample solution of M-0, M-10, M-100, M-200, and M-500.

2.3. Device Characterization. J-V curves were obtained by using J-V test system which consisted of solar simulator (100 mW/cm^2 AM 1.5), irradiance meter, electrochemical workstation (Linear Scan Voltammetry mode), test software, and so on (Figure 2). IPCE measurements were obtained with a IPCE measurement tool (0.3–0.8 mW/cm^2, 350–800 nm) developed by Institute of Physics, CAS, through DC method. EIS was measured with Princeton Applied Research, V3-400 electrochemical workstation equipped with electrochemical impedance test system. The bias was −0.5 V, the scanning frequency was from 0.1 Hz to 500 KHz, and the amplitude modulation was 20 mV.

3. Results and Discussions

3.1. Effect of Different Doping Concentration of Mg on the Performance of CdS/Mg-CdSe Quantum Dots Cosensitized Solar Cells. Because of the different doping concentration of Mg, some doped cells performed better than undoped cells, while some did not (Figure 1). The short-circuit current, fill factor, and efficiency of the cells increased first and then reduced (Table 1) with the decrease of doping concentration (from 1 : 10 to 1 : 500). Mg exited in CdSe QDS as dopant,

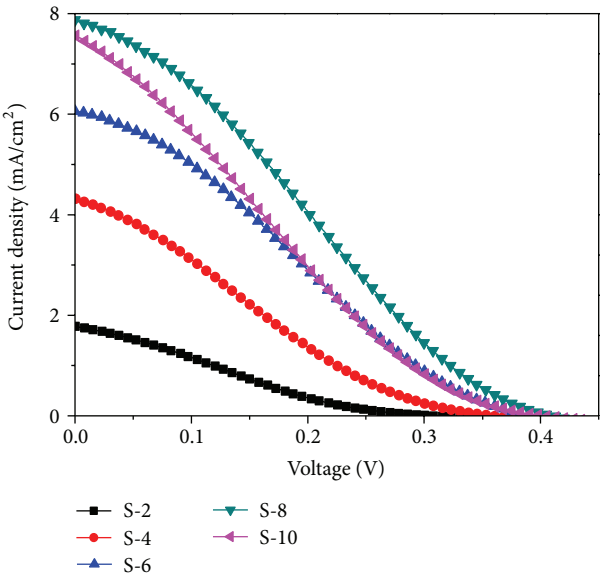

Figure 2: The J-V curves of samples of S-2, S-4, S-6, S-8, and S-10.

Table 1: The performance parameters of cells made by sample solution of M-0, M-10, M-100, M-200, and M-500.

Samples	J_{sc} (mA/cm^2)	V_{OC} (V)	FF	η (%)
M-0	4.17	0.42	0.35	0.61
M-10	4.82	0.44	0.32	0.68
M-100	5.24	0.43	0.34	0.77
M-200	5.66	0.44	0.34	0.85
M-500	4.40	0.41	0.32	0.57

M-0 stands for that the doping concentration of Mg is 0; similarly, M-10, M-100, M-200, and M-500, respectively, stand for the doping concentration of Mg (Mg : Cd) of 1 : 10, 1 : 100, 1 : 200, and 1 : 500. Each sample was deposited with 4 SILAR cycles of CdS followed by 4 SILAR cycles of Mg-CdSe.

which not only enhanced the short-circuit current density, but also decreased the short-circuit current density as it became the recombination center of electrons and holes. When the concentration of Mg was 1 : 200, we got the optimal result between the two factors. And because of the recombination centers introduced by dopant Mg, the open-circuit voltage did not change significantly.

3.2. Effect of Different SILAR Cycles of CdS on the Performance of CdS/Mg-CdSe Quantum Dot Cosensitized Solar Cells. We studied the effect of different SILAR cycles on the performance of CdS/Mg-CdSe quantum dot cosensitized solar cells after we got the best doping ratio (Mg : Cd = 1 : 200). The short-circuit current and open-circuit voltage (Table 2) keep increasing until the SILAR cycles of CdS are 8 and get to the maximum value of 7.87 mA/cm^2 and 0.41 V, respectively. However, the maximum efficiency of 0.84% was not further improved than previous experimental data. There might have been some problems in the preparation of TiO_2 films or Pt counter electrode. But the optimization of SILAR cycles of CdS has been shown in this experiment.

Table 2: The performance parameters of samples of S-2, S-4, S-6, S-8, and S-10.

Samples	J_{sc} (mA/cm^2)	V_{OC} (V)	FF	η (%)
S-2	1.79	0.31	0.22	0.12
S-4	4.31	0.36	0.22	0.34
S-6	6.06	0.39	0.26	0.61
S-8	7.87	0.41	0.26	0.84
S-10	7.55	0.40	0.22	0.65

S-2 means that the deposition cycles of CdS were 2. Similarly, S-4, S-6, S-8, and S-10 mean the deposition cycles of CdS were 4, 6, 8, and 10, respectively. All the deposition cycles of Mg-CdSe were 4.

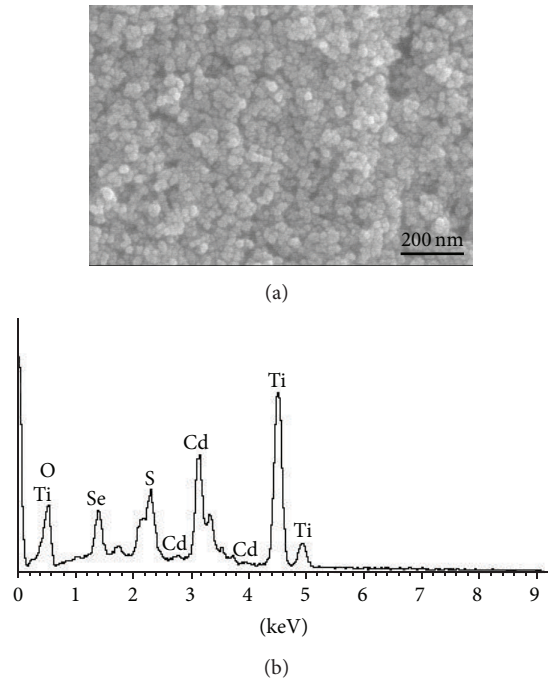

Figure 3: (a) The SEM image and (b) the EDS spectra of photoanode.

3.3. Analysis of Mg-CdSe Effecting the Performance of CdS/CdSe Quantum Dot Cosensitized Solar Cells. We found that Mg-doped CdSe had a great enhancement on the performance of CdS/CdSe quantum dot cosensitized solar cells (Figure 1). Here we analyze the mechanism of Mg-CdSe effecting the performance of CdS/CdSe quantum dot cosensitized solar cells specifically.

3.3.1. The Material Characterization of CdS/Mg-CdSe Photoanode. As we can see from the scanning electron microscopy (SEM) image of photoanode (Figure 3(a)), the size of TiO_2 is about 20 nm. However, it is hard to find the quantum dots in the SEM image. So we used transmission electron microscopy (TEM) to characterize the quantum dots.

Furthermore, we could not find element Mg in the energy dispersive spectroscopy (EDS) spectra (Figure 3(b)) of photoanode because the weight of $MgCl_2 \cdot 6H_2O$ was too little for just 0.0051 g to detect characteristic X-rays of

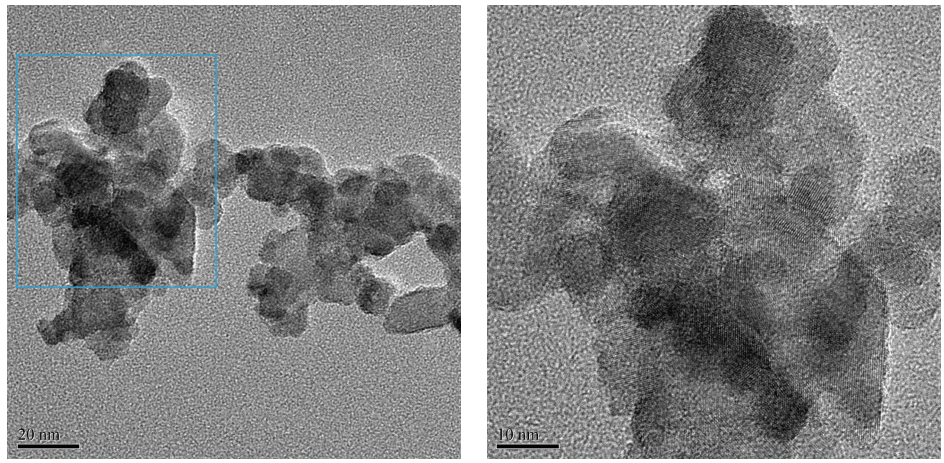

(a) (b)

Figure 4: TEM images of (a) low magnification and (b) high magnification.

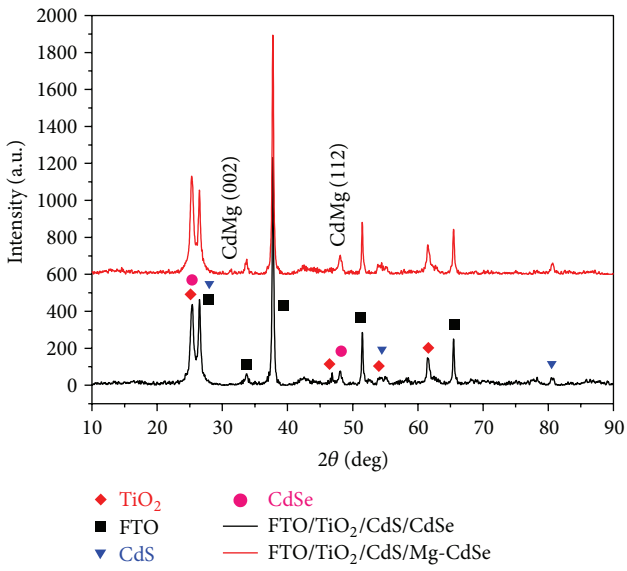

Figure 5: XRD pattern of CdS/Mg-doped CdSe photoanode.

Table 3: Quantitative analysis of ICP-OES.

Sample	Cd (μg)	Mg (μg)	Molar ratio (Mg : Cd)
Mg-CdSe	25.51	0.0299	0.54%

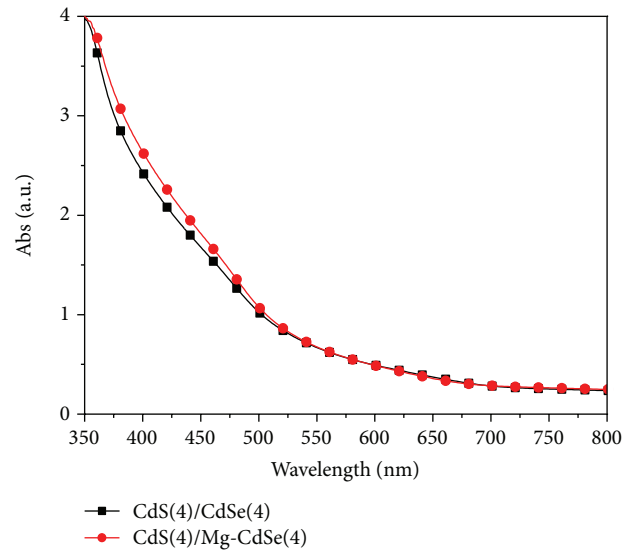

Figure 6: UV-Vis absorption spectroscopy of CdS(4)/Mg-CdSe(4) and CdS(4)/CdSe(4).

element Mg. So as to analyze element Mg qualitatively and quantitatively, we used inductively coupled plasma optical emission spectroscopy.

The size of nanoparticles is about 5–20 nm (Figure 4(a)). Furthermore, the smaller particles of Mg-doped QDs that were found, which are the size of 5 nm, are on the surface of bigger particles of TiO_2 (Figure 4(b)).

XRD results (Figure 5) show that the CdS/Mg-CdSe photoanode has a diffraction peak from impurity atoms of Mg except for diffraction peaks of FTO, TiO_2, CdS, and CdSe. Two peaks corresponding to lattice plane (002) and (112) of CdMg have been identified at 33.8° and 48.1°, respectively. Particularly, the peak of CdSe at 48.1° has been a little left shifted by 0.01° (from 48.10739° to 48.09740°) through lattice distortion caused by doping with Mg and it is very likely that the peak of TiO_2 at 46.8° has disappeared after being covered with quantum dots. So the element Mg dose has doped inside photoanode.

In order to further determine if the element Mg has doped into CdSe QDs, we analyzed quantitatively with ICP-OES (Table 3).

The experimental doping concentration of Mg was 0.5% (Mg : Cd = 1 : 200). However, the molar ratio of Mg : Cd was 0.54% actually. That was higher than the experimental data. It might be because the Mg ions reacted with Se ions more easily.

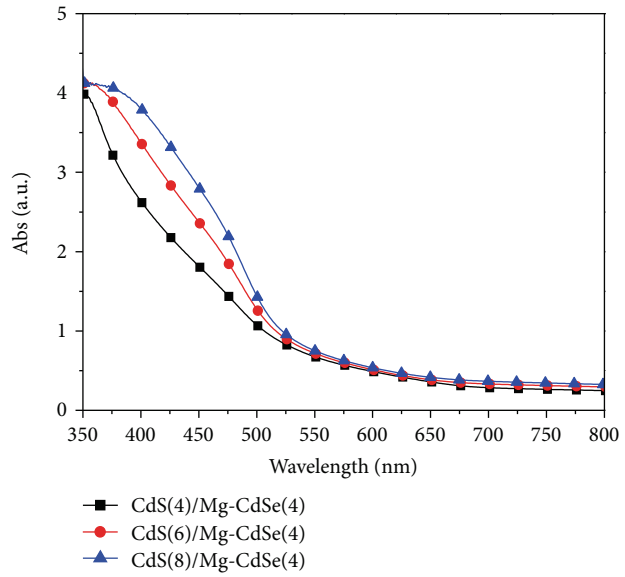

Figure 7: UV-Vis absorption spectroscopy of CdS/Mg-CdSe photoanode of different SILAR cycles.

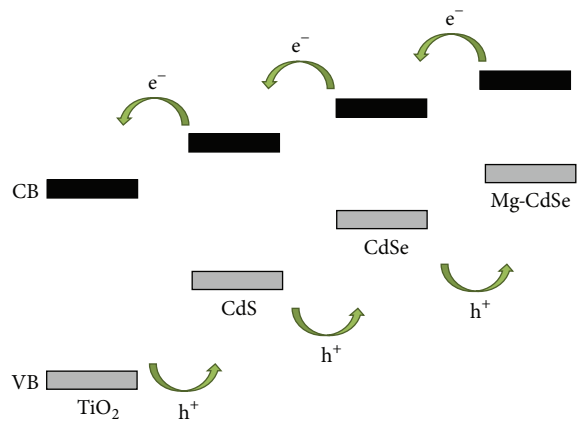

Figure 8: Energy level alignment by doping CdSe with Mg.

The comparison between absorption spectroscopy of CdS(4)/Mg-CdSe(4) and that of CdS(4)/CdSe(4) in UV-Vis (Figure 6) shows that the absorption of Mg-doped photoanode has performed a little better than undoped photoanode in the wavelength ranging from 350 nm to 525 nm according to the enhancement of current concentration.

As the deposition cycles of CdS were not optimal, we measured the absorption spectroscopy of CdS/Mg-CdSe photoanode with different SILAR cycles (Figure 7). The absorption of photoanode has been improved with the increasing of SILAR cycles from 4 to 8 in the same wavelength range when the deposition cycles of Mg-CdSe are 4, especially in the wavelength of 350–500 nm.

According to the UV-Vis absorption spectroscopy, the band-gap of CdSe has been narrowed by doping with Mg. Then we made a possible diagram (Figure 8) of the adjustment of Mg-CdSe energy level [6, 9]. The conduction band

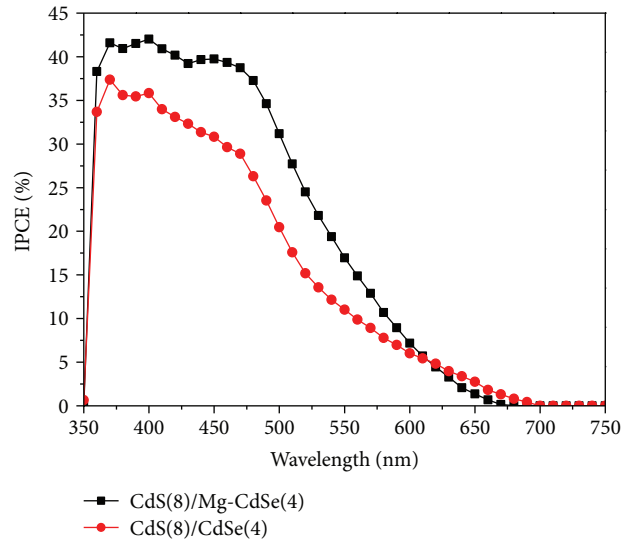

Figure 9: IPCE curves of cells made by the photoanode of CdS(8)/Mg-CdSe(4) and CdS(8)/CdSe(4), respectively.

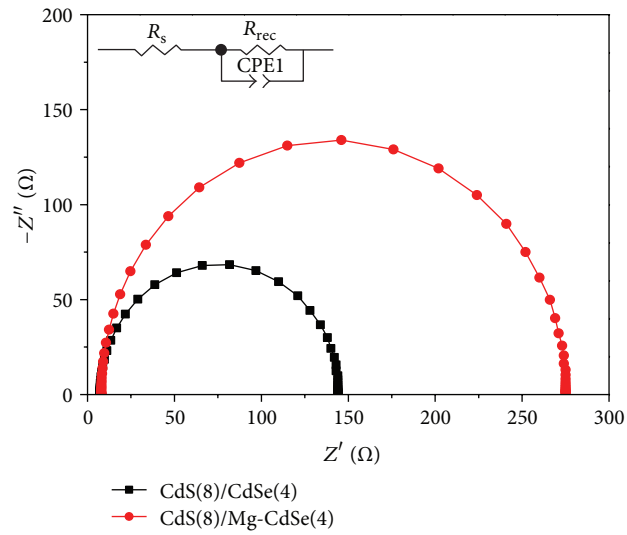

Figure 10: EIS of cells with the photoanode of CdS(8)/Mg-CdSe(4) and CdS(8)/CdSe(4). R_s is the series resistance of TCO electrodes, CPE1 is chemical capacitor of photoanode, and ($R_{rec} = r_{rec}L$) is electron recombination resistance.

and the valence band of CdSe both have become higher after doping with Mg. The stepwise structure yielded by level adjustment has enhanced the electron injection and the hole-recovery and reduced the recombination between electrons and holes, that is, agreement with the improved photocurrent (Table 1). As a result, the conversion efficiency has been enhanced by doping CdSe with Mg.

3.3.2. The Performance of Cells. The maximum value of IPCE has been improved after doping CdSe with Mg (Figure 9). In particular, the max value of IPCE has been improved from 37% to 42% in the wavelength of 350–475 nm. This has been

Table 4: Parameters of EIS before and after doping.

Sample number	R_s (Ω)	R_{rec} (Ω)	CPE1 (μF)
CdS(8)/CdSe(4)	7.17	137.2	10.65
CdS(8)/Mg-CdSe(4)	7.92	267.4	14.54

consistent with the improvement of preceding absorption spectrum and current density.

The electrochemical impedance spectroscopy (EIS) and the impedance fitting circuit diagram of photoanode and electrolyte are shown in Figure 10. The larger the R_{rec}, the smaller the electron concentration of photoanode and the recombination rate, and the greater the radius of the curves. So the recombination resistance has been increased by doping with Mg (Table 4).

Furthermore, the relationship of lifetime of electrons (τ) between chemical capacitor (CPE1) and electron recombination resistance (R_{rec}) is summarized as

$$\tau = \text{CPE1} \cdot R_{rec}. \quad (1)$$

The lifetime of electrons of CdS/Mg-CdSe system has been extended by doping CdSe with Mg compared with that of CdS/CdSe system.

As the performance of cells is decided by several kinds of factors, although this new attempt did not produce a high energy conversion efficiency (0.84%), we believe that we will get a high performance cell after overall optimization of cells.

4. Conclusions

Because of the doping with Mg, the stepwise structure which has improved the electron injection and the hole-recovery has been yielded. And the absorbance has been enhanced. The lifetime of electrons has also been extended. Thus the performance of cells has been improved by doping CdSe with Mg effectively.

Conflict of Interests

The authors declare that there is no conflict of interests regarding the publication of this paper.

Acknowledgments

This work was partially supported by Key Project of Beijing Natural Science Foundation (3131001), Key Project of Natural Science Foundation of China (91233201 and 61376057), Key Project of Beijing Education Committee Science & Technology Plan (KZ201211232040), State 863 Plan of MOST of China (2011AA050527), Beijing National Laboratory for Molecular Sciences (BNLMS2012-21), State Key Laboratory of Solid State Microstructures of Nanjing University (M27019), State Key Laboratory for New Ceramic and Fine Processing of Tsinghua University (KF1210), Key Laboratory for Renewable Energy and Gas Hydrate of Chinese Academy of Sciences (y207ka1001), Beijing Key Laboratory for Sensors of BISTU (KF20141077207 and KF20141077208), and Beijing Key Laboratory for photoelectrical measurement of BISTU (GDKF2013005).

References

[1] J.-W. Lee, D.-Y. Son, T. K. Ahn et al., "Quantum-dot-sensitized solar cell with unprecedentedly high photocurrent," *Scientific Reports*, vol. 3, article 1050, 2013.

[2] W.-C. Kwak, K. T. Geun, W.-S. Chae, and Y.-M. Sung, "Tuning the energy bandgap of CdSe nanocrystals via Mg doping," *Nanotechnology*, vol. 18, no. 20, 2007.

[3] Y.-M. Sung, W.-C. Kwak, W. Kim, and T. G. Kim, "Enhanced ripening behavior of Mg-doped CdSe quantum dots," *Journal of Materials Research*, vol. 23, no. 7, pp. 1916–1921, 2008.

[4] L. Wonjoo, K. Woo-Chul, M. S. Ki et al., "Spectral broadening in quantum dots-sensitized photoelectrochemical solar cells based on CdSe and Mg-doped CdSe nanocrystals," *Electrochemistry Communications*, vol. 10, no. 11, pp. 1699–1702, 2008.

[5] Y.-C. Wang, M. Wang, X.-Y. Su, Z.-Y. Li, and W. Zhao, "First-principles on the electron structure and optical properties of the Mg-doped CdSe system," *Chinese Journal of Luminescence*, vol. 31, no. 6, pp. 842–847, 2010.

[6] Y.-L. Lee and Y.-S. Lo, "Highly efficient quantum-dot-sensitized solar cell based on co-sensitization of CdS/CdSe," *Advanced Functional Materials*, vol. 19, no. 4, pp. 604–609, 2009.

[7] Z. Huang, X. Zou, and H. Zhou, "A strategy to achieve superior photocurrent by Cu-doped quantum dot sensitized solar cells," *Materials Letters*, vol. 95, pp. 139–141, 2013.

[8] L. Li, X. Zou, H. Zhou, and G. Teng, "Cu-doped-CdS/In-doped-CdS cosensitized quantum dot solar cells," *Journal of Nanomaterials*, vol. 2014, Article ID 314386, 8 pages, 2014.

[9] X. Zou, S. He, G. Teng, and C. Zhao, "Performance study of CdS /Co-doped- CdSe quantum dot sensitized solar cells," *Journal of Nanomaterials*, vol. 2014, Article ID 818160, 6 pages, 2014.